Computational Mechanics 26 (2000) 333–343 © Springer-Verlag 2000

Meshless methods based on collocation with radial basis functions*

X. Zhang, K. Z. Song, M. W. Lu, X. Liu

Abstract Meshless methods based on collocation with radial basis functions (RBFs) are investigated in detail in this paper. Both globally supported and compactly supported radial basis functions are used with collocation to solve partial differential equations (PDEs). Using RBFs as a meshless collocation method to solve PDEs possesses some advantages. It is a truly mesh-free method, and is space dimension independent. Furthermore, in the context of scattered data interpolation it is known that some radial basis functions have spectral convergence orders.

This study shows that the accuracy of derivatives of interpolating functions are usually very poor on boundary of domain when a direct collocation method is used, therefore it will result in significant error in solving a PDE with Neumann boundary conditions. Based on this fact, a Hermite type collocation method is proposed in this paper, in which both PDEs and prescribed traction boundary conditions are imposed on prescribed traction boundary. Numerical studies shows that the Hermite type collocation method improve the accuracy significantly.

1 Introduction

During the past thirty years, the numerical solution of partial differential equations (PDEs) has commonly been obtained by using the finite element methods (FEM) and finite difference methods (FDM). However, the lack for robust and efficient 3D mesh generators makes the solution of 3D problems a difficult task. Furthermore, mesh-based methods are also not well suited to the problems associated with extremely large deformation and problems associated with frequency remeshing. To avoid these drawbacks of the FEM and DEM, considerable effort has been devoted during recent years to the development of the so-called meshless method, and about 10 different meshless methods have been developed, such as the Smooth Particle Hydrodynamics (SPH) [1], the Element-free Galerkin (EFG) method [2], the Reproducing Kernel Particle (RKP) method [3], the Finite Point (FP) method [4], the hp clouds method [5], Meshless Local Petrov–Galerkin (MLPG) [6–9], Local Boundary Integral Equation (LBIE) [7–11], and several others.

Two methods of discretization, collocation methods and Galerkin methods, have been dominant in existing meshless methods. One of the major difficulties in the implementation of Galerkin-based meshless method is the noninterpolatory character of the approximation. As a consequence, the imposition of essential boundary conditions is quite awkward and several approaches have been developed [8, 12–16]. Furthermore, in many Galerkin-based meshless methods, recourse must be taken to meshes for the purpose of quadrature, so they are not truly meshless methods. In contrast, collocation-based meshless are truly meshless methods, and are very efficient.

The radial basis functions (RBFs) have been successfully developed for multivariate interpolation. Frank [17] compared the results of 29 scattered data interpolation methods, and showed that Hardy's multiquadric (MQ) [18] and Duchon's thin-plate spline (TPS), two of special class of RBFs, methods were ranked the best in accuracy. Wu [19] proved existence and characterization theorems for Hermite-Birkhoff interpolation of scattered multidimensional data by radial basis function. Recently, Kansa [20, 21] introduced the concept of solving PDEs using RBFs with collocation for hyperbolic, parabolic, and elliptic types. Both Kansa [21], Sharan et al. [22] showed dramatic efficiencies with the exponentially convergent MQ scheme. In Kansa's collocation method, the stiffness matrix is unsymmetric. Fasshauer [23] reported an Hermite-based approach which results in a (anti-)symmetric stiffness matrix for some special PDEs. Wu et al. [24, 25] and Franke et al. [26] provided the convergence proofs and error estimations in applying the RBFs for scattered data interpolation and solving PDEs.

Using RBFs as a meshless collocation method to solve PDEs possesses some advantages: (1) it is a truly mesh-free algorithm; (2) it is space dimension independent in the sense that the convergence order is of $O(h^{d+1})$ where h is the density of the collocation points and d is the spatial dimension; and (3) in the context of scattered data interpolation it is known that some radial basis functions have spectral convergence orders (e.g., (reciprocal) multiquadrics, Gaussians). This should also be evident in some form when using them for collocation. However, radial basis functions are generally globally supported and poorly conditioned. There are currently several ways to overcome these disadvantages of using RBFs for solving PDEs, such as domain decomposition [27], preconditioning, and fine tuning of the shape parameter of MQ. Compactly

Received 31 January 2000

X. Zhang (✉), K. Z. Song, M. W. Lu, X. Liu
Department of Engineering Mechanics, Tsinghua University, Beijing 100084, P.R. China

*Supported by the National Natural Foundation of China under grant number 19772024

supported RBFs provide a promising approach [28–30]. Wu [28] provided criteria for positive definiteness of radial functions with compact supports and produced a series of positive definite and compactly supported radial functions. Buhmann [30] studied compactly supported positive definite radial functions which are related to the well-known thin spline radial functions. Wendland's [29] functions are similar to those given by Wu, but of minimal degree.

In the existing literature, most studied on radial basis functions are based on the computational mathematics point of view. In this paper, meshless methods based on collocation with compactly supported RBFs are investigated and numerical results are compared with those obtained by using collocation with global supported RBFs, such as MQ and TPS. A Hermite type collocation method is also proposed, which improve the accuracy significantly. In this Hermite type collocation method, degrees of freedom corresponding to tractions at prescribed traction boundary nodes are taken as independent variables, and both PDEs and boundary conditions are imposed at these boundary nodes.

This paper is organized as follows. In Sect. 2, basic idea of RBFs are given, and scattered data interpolation by compactly supported RBFs is studied. It shows that interpolation by the RBFs performs very excellent in the inner region, but it results in significant error at boundary nodes. Consequently, using collocation with RBFs to solve a PDE with Neumann boundary conditions could results in significant error. This conclusion should also be valid to any interpolation method based on collocation. Based on this consideration, a Hermite type interpolation is proposed, and the accuracy is improved significantly. In Sect. 3, meshless methods based on direct collocation (DC) and Hermite type collocation (HC) with compactly supported RBFs are studied. In Sect. 4, as a test on the proposed meshless methods, a Poisson equation, a cantilevered beam and a infinite plate with a hole are studied. In Sect. 5, some concluding remarks are discussed.

2
Scattered data interpolation by compactly supported radial basis functions

For scattered $(\mathbf{x}_i, f_i) \in \mathbf{R}^{d+1}$, radial basis function interpolation methods use a "radial" function $\varphi : \mathbf{R}^d \to \mathbf{R}$ to construct the interpolant g satisfying $g(\mathbf{x}_i) = f_i$ as

$$g(\mathbf{x}) = \sum_{k=1}^{N} c_k \varphi(\|\mathbf{x} - \mathbf{x}_k\|) \ , \tag{1}$$

where the norm $\|\cdot\|$ in Euclidean, $\varphi(\|\mathbf{x} - \mathbf{x}_k\|)$ is referred to as radial basis functions centered at $\mathbf{x}_k$, which are called centers or sometimes knots. In this paper, they are also referred to as nodes. The solution of this problem leads to a linear system $\mathbf{Ac} = \mathbf{f}$ with the entries of $\mathbf{A}$ given by

$$A_{jk} = \varphi(\|\mathbf{x}_j - \mathbf{x}_k\|), \quad j,k = 1,2,\ldots,N$$

Clearly, there exists a unique solution if and only if $\mathbf{A}$ is non-singular. Micchelli [31] and Powell [32] have shown the existence of the interpolation (1) for standard radial basis functions. If globally supported radial basis functions are used, the coefficient matrix $\mathbf{A}$ will be a full matrix and poorly conditioned. However, $\mathbf{A}$ will be a sparse matrix and positive definite if compactly supported positive definite radial functions are used [28–30]. The compactly supported positive definite RBFs studied in this paper are:

$$\left.\begin{array}{ll}
\text{CSRBF1:} & (1-r)_+^4(4+16r+12r^2+3r^3) \in C^2 \cap PD_3 \\
\text{CSRBF2:} & (1-r)_+^6(6+36r+82r^2+72r^3+30r^4 \\
 & \qquad +5r^5) \in C^4 \cap PD_3 \\
\text{CSRBF3:} & \frac{1}{3}+r^2-\frac{4}{3}r^3+2r^2\ln r \quad \text{if } 0 \le r \le 1 \\
\text{CSRBF4:} & \frac{1}{15}+\frac{19}{6}r^2-\frac{16}{3}r^3+3r^4-\frac{16}{15}r^5+\frac{1}{6}r^6+2r^2\ln r \\
 & \qquad \text{if } 0 \le r \le 1 \\
\text{CSRBF5:} & (1-r)_+^6(35r^2+18r+3) \in C^4 \cap PD_3 \\
\text{CSRBF6:} & (1-r)_+^8(32r^3+25r^2+8r+1) \in C^6 \cap PD_3
\end{array}\right\} \tag{2}$$

where $r = \|x\|$, PD_d represents that the radial function is positive definite in $\mathbf{R}^d$, and $(1-r)_+$ is given by

$$(1-r)_+ = \begin{cases} (1-r) & \text{if } 0 \le r \le 1 \\ 0 & \text{otherwise} \end{cases}$$

Amongst these radial functions, CSRBF1 and CSRBF2 are proposed by Wu [28], CSRBF3 and CSRBF4 are proposed by Buhmann [30], CSRBF5 and CSRBF6 are proposed by Wendland [29].

The size of support for radial functions listed in (2) equals 1. In a practical application, a transformation,

$$r = \|\mathbf{x}\| = \sqrt{\left(\frac{x}{R_x}\right)^2 + \left(\frac{y}{R_y}\right)^2} \tag{3}$$

can be used to define the support for the radial functions. The support of node x_k defined by (3) is an ellipse if $R_x \neq R_y$. In this paper, we assume that $R_x = R_y = R$.

For comparison, the globally supported RBFs

$$\left.\begin{array}{l}
\text{Multiquadrics (MQ):} \ \ (c^2+r^2)^{1/2}, \ c>0 \\
\text{Reciprocal multiquadrics (RMQ):} \ \ (c^2+r^2)^{-1/2}, \ c>0 \\
\text{Gaussians:} \ \ \exp(-cr^2), \ c>0 \\
\text{Thin-plate splines (TPS):} \ \ r^{2\beta}\log r, \ \beta \in \mathbf{N}
\end{array}\right\} \tag{4}$$

are also used in this paper.

To compare the accuracy of interpolation using different radial functions, the function

$$f(x,y) = \sin(x)\cos(y) \quad x \in [0.5, 3.0], \ y \in [0.5, 3.0]$$

is interpolated using RBFs given by (2) and (4). To avoid using background cells for quadrature, the relative error in the first order derivatives and in the second order derivatives of $g(x)$ are calculated by

$$E_2 = \frac{\sqrt{\sum_{k=1}^{N}(\mathrm{d}\mathbf{g}-\mathrm{d}\mathbf{f})^{\mathrm{T}}(\mathrm{d}\mathbf{g}-\mathrm{d}\mathbf{f})}}{\sqrt{\sum_{k=1}^{N}\mathrm{d}\mathbf{f}^{\mathrm{T}}\mathrm{d}\mathbf{f}}} \times 100\% \tag{5}$$

$$D_2 = \frac{\sqrt{\sum_{k=1}^{N}(\mathrm{d}^2\mathbf{g}-\mathrm{d}^2\mathbf{f})^{\mathrm{T}}(\mathrm{d}^2\mathbf{g}-\mathrm{d}^2\mathbf{f})}}{\sqrt{\sum_{k=1}^{N}\mathrm{d}^2\mathbf{f}^{\mathrm{T}}\mathrm{d}^2\mathbf{f}}} \times 100\% \tag{6}$$

where $\mathbf{df} = [f_{,x}, f_{,y}]^{\mathrm{T}}$, $\mathbf{dg} = [g_{,x}, g_{,y}]^{\mathrm{T}}$, $\mathrm{d}^2\mathbf{f} = [f_{,xx}, f_{,yy}, f_{,xy}]^{\mathrm{T}}$, $\mathrm{d}^2\mathbf{g} = [g_{,xx}, g_{,yy}, g_{,xy}]^{\mathrm{T}}$. In this test, a 10×10 regular nodes discretization is used. Table 1 presents the relative error E_2 and D_2 obtained by using compactly supported RBFs for various support size, while Table 2 presents those obtained by using globally supported RBFs. Because CSRBF3 and CSRBF4 only possess C^1 smoothness, the results for the second order of derivatives obtained by using these two functions are not acceptable, so that they are not presented in Table 1. Figures 1–6 show the relative error distribution in $g_{,x}$ and $g_{,xx}$ obtained by using the CSRBF2 and CSRBF6 with $R = 4.0$ and MQ with $c = 2.0$, respectively. This study shows that all globally supported RBFs possess excellent accuracy, while the accuracy of the compactly supported RBFs increase with the increasing of the support size. However, even all data points are included in the support of an interpolation point, the accuracy of compactly supported RBFs is still much worse than that of the globally supported RBFs.

Table 1. Relative error obtained by using compactly supported RBFs (%)

	R	CSRBF1	CSRBF2	CSRBF3	CSRBF4	CSRBF5	CSRBF6
E_2	1.0	27.6	33.8	38.5	66.8	44.7	56.3
	2.0	6.22	4.90	13.7	33.5	7.90	7.92
	3.0	3.36	1.46	8.34	19.5	2.65	2.00
	4.0	2.21	0.79	7.09	13.6	1.34	0.76
D_2	1.0	301	328	–	–	427	513
	2.0	71.1	54.1	–	–	86.3	90.2
	3.0	38.3	17.3	–	–	30.5	24.9
	4.0	25.1	9.53	–	–	15.8	9.82

Table 2. Relative error obtained by using globally supported RBFs (%)

	MQ ($c = 3$)	MQ ($c = 6$)	RMQ ($c = 3$)	RMQ ($c = 6$)	Gaussians ($c = 0.2$)	Gaussians ($c = 0.5$)	TPS ($\beta = 4$)
E_2	0.006	0.0008	0.011	0.0018	0.003	0.014	0.20
D_2	0.11	0.01	0.188	0.024	0.04	0.224	3.16

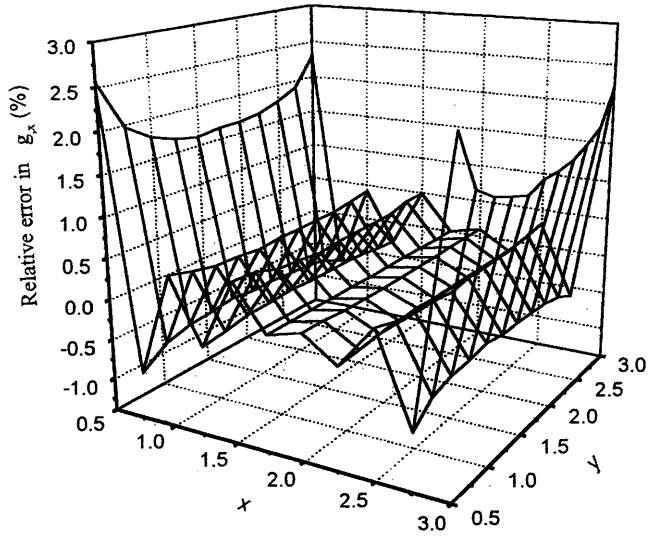

Fig. 1. Relative error distribution in $g_{,x}$ obtained by using the CSRBF2 with $R = 4$

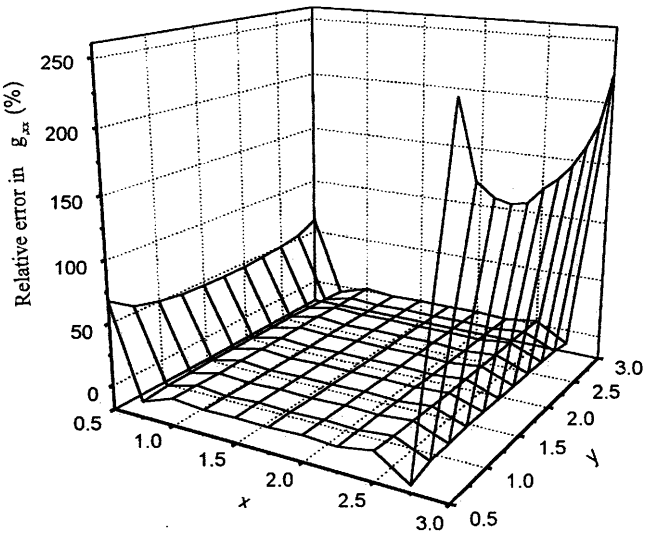

Fig. 2. Relative error distribution in $g_{,xx}$ obtained by using the CSRBF2 with $R = 4$

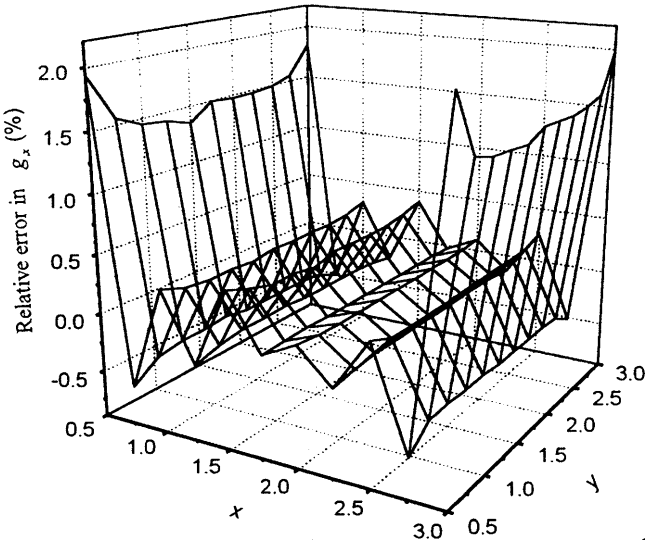

Fig. 3. Relative error distribution in $g_{,x}$ obtained by using the CSRBF6 with $R = 4$

Because collocation method is used, the interpolation using the radial functions perform very excellent in the inner region, but results in significant error in derivatives at all boundary points, as shown in Figs. 1–6. Consequently, using collocation with the RBFs to solve a PDE could result in significant error due to the inaccurate approximation of derivatives at boundary points. From this point of view, an Hermite interpolation is desirable. Assume that data $\{\mathbf{x}_j, f(\mathbf{x}_j)\}_{j=1}^{n}$ and $\{\mathbf{x}_j, f_{,x}(\mathbf{x}_j)\}_{j=n+1}^{N}$ with $\mathbf{x} = (x, y) \in \mathbf{R}^2$ be given, the interpolant g can be constructed as

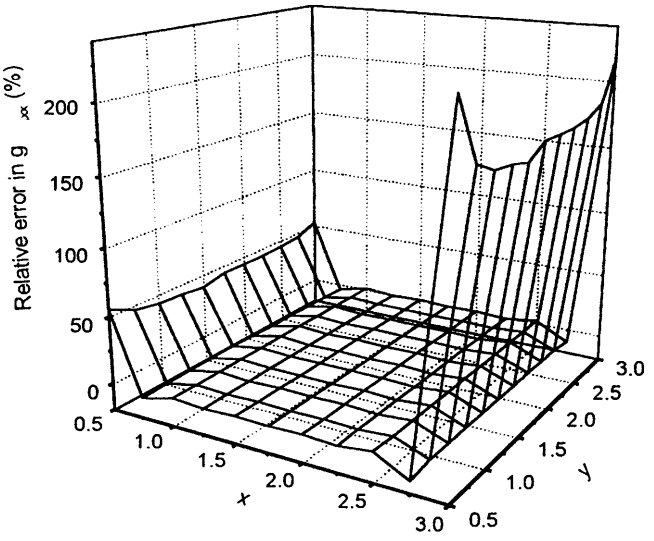

Fig. 4. Relative error distribution in $g_{,xx}$ obtained by using the CSRBF6 with $R = 4$

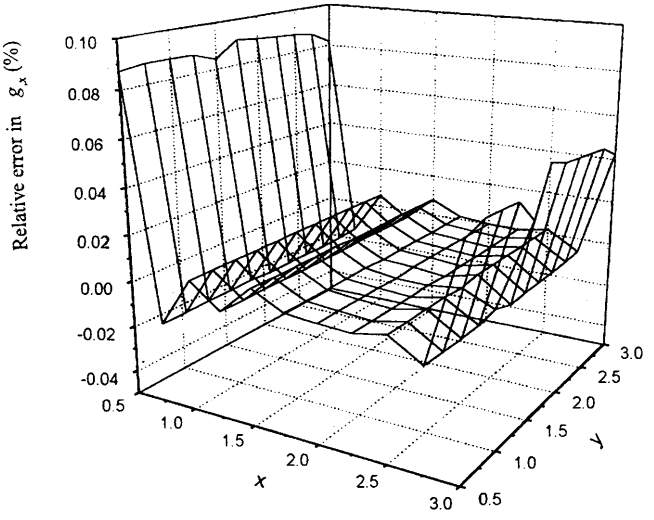

Fig. 5. Relative error distribution in $g_{,x}$ obtained by using the MQ with $c = 2$

$$g(\mathbf{x}) = \sum_{k=1}^{n} c_k \varphi(\|\mathbf{x} - \mathbf{x}_k\|) + \sum_{k=n+1}^{N} c_k \frac{\partial \varphi}{\partial \mathbf{x}}(\|\mathbf{x} - \mathbf{x}_k\|) \ . \quad (7)$$

where n is the total number of inner nodes. The solution of this problem leads to a linear system $\mathbf{Ac} = \mathbf{f}$ with the entries of $\mathbf{A}$ given by

$$A = \begin{bmatrix} \Phi & \Phi_x \\ \Phi_x & \Phi_{xx} \end{bmatrix} \ , \quad (8)$$

and

$$\Phi_{jk} = \varphi(\|\mathbf{x}_j - \mathbf{x}_k\|), \quad j,k = 1,2,\ldots,n,$$

$$\Phi_{x,jk} = \frac{\partial \varphi}{\partial \mathbf{x}}(\|\mathbf{x}_j - \mathbf{x}_k\|), \quad j = 1,2,\ldots,n, k = n+1,\ldots,N,$$

$$\Phi_{xx,jk} = \frac{\partial^2 \varphi}{\partial \mathbf{x}^2}(\|\mathbf{x}_j - \mathbf{x}_k\|), \quad j,k = n+1,\ldots,N \ .$$

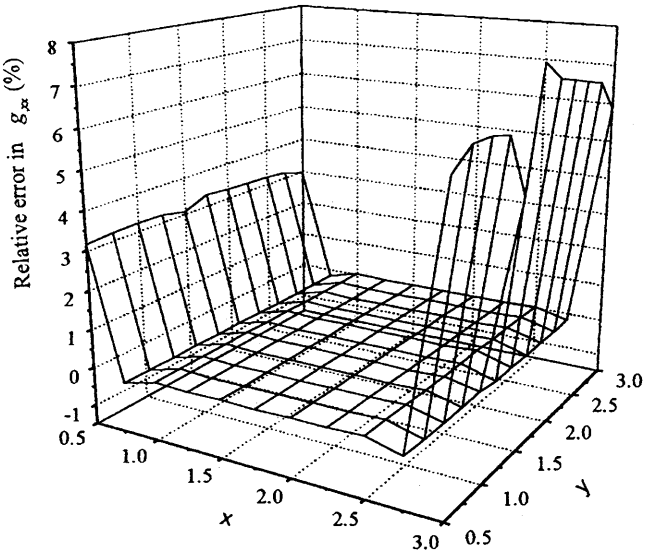

Fig. 6. Relative error distribution in $g_{,xx}$ obtained by using the MQ with $c = 2$

Tables 3 and 4 present the relative error E_2 and D_2 obtained by using the Hermite type interpolation with the RBFs. This test shows that the accuracy of derivatives is improved significantly by using the Hermite type interpolation, so we can expect that the accuracy will also be improved significantly by using the Hermite type interpolation in solving a PDE. Note that the performance of the global RBFs are largely depended on the parameter c for MQ, RMQ and Gaussians, and on β for TPS. An optimized parameter has not been obtained and it is problem dependent.

3
Collocation with compactly supported RBFs

Consider the elasticity problem

$$\mathbf{A}\sigma = -\mathbf{f}(x,y), \text{ in } \Omega \ , \quad (9)$$

$$\mathbf{u} = \bar{\mathbf{u}}, \text{ on } \Gamma_u \ , \quad (10)$$

$$\mathbf{n}\sigma = \bar{\mathbf{t}}, \text{ on } \Gamma_t \ , \quad (11)$$

where

$$\mathbf{A} = \begin{bmatrix} \frac{\partial}{\partial x} & 0 & \frac{\partial}{\partial y} \\ 0 & \frac{\partial}{\partial y} & \frac{\partial}{\partial x} \end{bmatrix}, \quad \mathbf{n} = \begin{bmatrix} l & 0 & m \\ 0 & m & l \end{bmatrix},$$

$$\sigma = [\,\sigma_{xx} \quad \sigma_{yy} \quad \tau_{xy}\,]^{\mathrm{T}}, \quad \mathbf{u} = [\,u \quad v\,]^{\mathrm{T}},$$

Table 3. L_2 relative error norm obtained by using Hermite interpolation with compactly supported RBFs (%)

	R	CSRBF1	CSRBF2	CSRBF3	CSRBF4	CSRBF5	CSRBF6
E_2	1.0	10.3	4.58	37.1	65.2	25.2	37.1
	2.0	0.36	0.51	11.3	32.7	0.68	0.65
	3.0	0.23	0.19	6.30	18.1	0.33	0.24
	4.0	0.12	0.07	4.90	11.8	0.15	0.10
D_2	1.0	220	108	–	–	183	216
	2.0	43.0	24.3	–	–	41.1	38.2
	3.0	24.1	7.92	–	–	14.5	10.2
	4.0	15.1	3.83	–	–	6.90	3.73

Table 4. L_2 relative error norm obtained by using Hermite interpolation with globally supported RBFs (%)

	MQ ($c = 3$)	MQ ($c = 6$)	RMQ ($c = 3$)	RMQ ($c = 6$)	Gaussians ($c = 0.2$)	Gaussians ($c = 0.5$)	TPS ($\beta = 4$)
E_2	5.7×10^{-5}	1.0×10^{-4}	1.4×10^{-4}	1.5×10^{-4}	3.35×10^{-4}	3.95×10^{-4}	0.034
D_2	0.006	0.0018	0.0069	0.0015	0.008	0.015	1.20

and l, m are the direction cosines of the outward normal direction of boundary Γ_t. Equations (9)–(11) can be expressed in displacement vector $\mathbf{u}$ as

$$\mathbf{Gu} = -\mathbf{f}(x,y), \text{ in } \Omega \ , \tag{12}$$

$$\mathbf{u} = \bar{\mathbf{u}}, \text{ on } \Gamma_u \ , \tag{13}$$

$$\mathbf{Tu} = \bar{\mathbf{t}}, \text{ on } \Gamma_t \ , \tag{14}$$

where

$$\mathbf{G} = \frac{E}{1-\nu^2}\begin{bmatrix} \frac{\partial^2}{\partial x^2} + \frac{1-\nu}{2}\frac{\partial^2}{\partial y^2} & \frac{1+\nu}{2}\frac{\partial^2}{\partial x \partial y} \\ \frac{1+\nu}{2}\frac{\partial^2}{\partial x \partial y} & \frac{\partial^2}{\partial y^2} + \frac{1-\nu}{2}\frac{\partial^2}{\partial x^2} \end{bmatrix},$$

$$\mathbf{T} = \frac{E_0}{1-\nu_0^2}\begin{bmatrix} l\frac{\partial}{\partial x} + m\frac{1-\nu}{2}\frac{\partial}{\partial y} & l\nu\frac{\partial}{\partial y} + m\frac{1-\nu}{2}\frac{\partial}{\partial x} \\ m\nu\frac{\partial}{\partial x} + l\frac{1-\nu}{2}\frac{\partial}{\partial y} & m\frac{\partial}{\partial y} + l\frac{1-\nu}{2}\frac{\partial}{\partial x} \end{bmatrix} .$$

In collocation method, the prescribed traction condition (11) needs to be explicitly implemented even on free boundaries where the prescribed traction vector is zero. This quite different to the Galerkin method, where free boundaries require no calculation of boundary integral.

3.1 Direct collocation

In direct collocation, the displacement vector $\mathbf{u}(x,y)$ is approximated by

$$\mathbf{u}(x,y) = \sum_{k=1}^{N} c_k \varphi(\|\mathbf{x} - \mathbf{x}_k\|) \ , \tag{15}$$

where $\varphi(\|\cdot\|)$ is the radial basis functions chosen from (2) and (4), and c_k are coefficients to be determined. Substituting (15) into (12)–(14) results in

$$\begin{bmatrix} \mathbf{G}[\Phi] \\ \Phi \\ \mathbf{T}[\Phi] \end{bmatrix} \cdot \mathbf{c} = \begin{bmatrix} -\mathbf{f} \\ \bar{\mathbf{u}} \\ \bar{\mathbf{t}} \end{bmatrix} \ , \tag{16}$$

where

$$\Phi_{jk} = \varphi(\|\mathbf{x}_j - \mathbf{x}_k\|) \ .$$

In the direct collocation, the coefficient matrix is unsymmetric. According to the numerical results presented in Sect. 2, using the direct collocation method will lead to significant error in the derivatives on boundaries, and the Hermite type interpolation could improve the accuracy significantly in solving PDE with Neumann boundary conditions. Furthermore, discretization of the boundary conditions (13) or (14) precludes discretizations of the PDE (12) at this node, consequently, the accuracy of the collocation method may be reduced. In this paper, an Hermite type collocation is developed.

3.2 Hermite type collocation

Assume that there are N_u nodes on Γ_u, N_t nodes on Γ_t, and $N_\Omega = N - N_u - N_t$ nodes in domain Ω. In the Hermite type interpolation, the displacement vector $\mathbf{u}$ is approximated by

$$\mathbf{u}(\mathbf{x}) = \sum_{k=1}^{N} \phi(\|\mathbf{x} - \mathbf{x}_k\|)\mathbf{c}_k + \sum_{k=1}^{N_t} \mathbf{T}[\phi(\|\mathbf{x} - \mathbf{x}_k\|)]\mathbf{c}_k \ , \tag{17}$$

where

$$\phi(\|\mathbf{x} - \mathbf{x}_k\|) = \begin{bmatrix} \varphi(\|\mathbf{x} - \mathbf{x}_k\|) & 0 \\ 0 & \varphi(\|\mathbf{x} - \mathbf{x}_k\|) \end{bmatrix} \ ,$$

$\mathbf{c}_k$ is a coefficient vector and $\mathbf{T}$ is the differential operator defined in (14). Note that additional degrees of freedom are introduced into (17) at all boundary nodes. In this procedure, both PDE (12) and prescribed traction conditions (14) are imposed at all nodes on boundary Γ_t. As a result, PDEs are satisfied at all inner nodes and boundary nodes on Γ_t.

Substituting (17) into (12)–(14) results in

$$\mathbf{KU} = \mathbf{P} \tag{18}$$

where

$$\mathbf{K} = \begin{bmatrix} \mathbf{G}[\Phi] & \mathbf{G}[\mathbf{T}[\Phi]] \\ [\Phi] & \mathbf{T}[\Phi] \\ \mathbf{T}[\Phi] & \mathbf{T}[\mathbf{T}[\Phi]] \end{bmatrix}, \qquad \mathbf{P} = \begin{bmatrix} -\mathbf{f} \\ \bar{\mathbf{u}} \\ \bar{\mathbf{t}} \end{bmatrix} \ ,$$

and $\mathbf{U}$ is a vector consist of $2 * (N + N_u + N_t)$ unknowns for a two-dimensional problem.

It is straightforward to impose PDEs at all boundary nodes including those on Γ_u, but our numerical studies

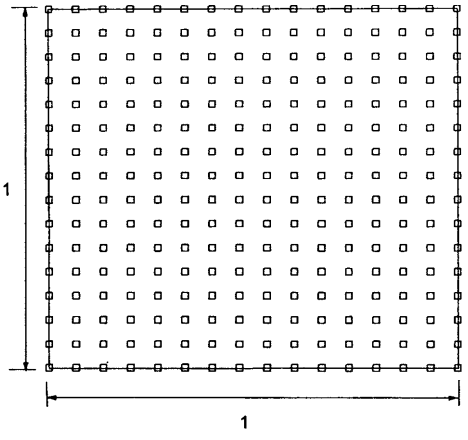

Fig. 7. A regular 15×15 nodes discretization for the Poission equation

show that better results are always obtained when PDEs are only imposed at boundary nodes on Γ_t.

4 Numerical examples

4.1 Poisson equation

As the first numerical example, the Poisson equation,

$$\Delta u(x,y) = -2*(x+y-x^2-y^2) \quad \text{in } \Omega: x\in[0,1],\ y\in[0,1]\ , \qquad (19)$$
$$u(x,y) = 0.0,\ \text{on } \partial\Omega\ ,$$

is studied. The exact solution is given by

$$u(x,y) = (x-x^2)(y-y^2)\ .$$

This problem is analyzed for a 15×15 regular and an irregular nodes discretization, as shown in Figs. 5 and 6. The numerical results are obtained for the regular and irregular nodes discretization by using the direct collocation and the Hermite type collocation with CSRBF2 and CSRBF6, and compared with those obtained by using MQ and TPS in Tables 5–7. Due to the poor performance of CSRBF3 and CSRBF4, only CSRBF2 and CSRBF6 are used in the following examples.

Convergence rates are studied by using $5\times 5, 10\times 10, 15\times 15, 20\times 20, 25\times 25$, and 30×30 regular nodes discretization and results are shown in Figs. 9–12.

Table 5. Relative error norm in u and in derivatives for the regular nodes discretization by using the direct collocation (%)

	R	CSRBF2	CSRBF6	MQ with $c=1$	TPS with $\beta=4$
L_2^u	0.25	12.1	20.3	0.0007	0.045
	0.5	1.34	1.78		
	1.0	0.45	0.45		
	1.5	0.23	0.18		
L_2^d	0.25	27.5	36.3	0.0071	0.352
	0.5	9.22	12.4		
	1.0	3.24	3.15		
	1.5	1.70	1.31		

Table 6. Relative error norm in u and in derivatives for the irregular nodes discretization by using direct collocation (%)

	R	CSRBF2	CSRBF6	MQ with $c=1$
L_2^u	0.25	58.4	81.0	0.003
	0.5	2.77	6.8	
	1.0	1.62	6.39	
	1.5	0.60	2.99	
L_2^d	0.25	63.4	83.6	0.015
	0.5	12.9	28.4	
	1.0	7.12	21.2	
	1.5	3.13	10.8	

Table 7. Relative error norm in u and in derivatives for the regular nodes discretization by using Hermite type collocation (%)

	R	CSRBF2	CSRBF6	MQ with $c=1$	TPS with $\beta=4$
L_2^u	0.25	7.34	15.0	0.001	0.002
	0.5	0.30	0.43		
	1.0	0.10	0.07		
	1.5	0.06	0.04		
L_2^d	0.25	19	48.6	0.002	0.002
	0.5	3.56	4.71		
	1.0	0.82	0.64		
	1.5	0.51	0.22		

4.2 Cantilered beam

The exact solution for cantilever beam subjected to end load as shown in Fig. 13 is given by Timoshenko and Goodier [33] as

$$\begin{cases} u_x = -\frac{P}{6EI}\left(y-\frac{D}{2}\right)[(6L-3x)x+(2+v)(y^2-Dy)] \\ u_y = \frac{P}{6EI}\left[3v\left(y-\frac{1}{2}D\right)^2(L-x)+\frac{1}{4}(4+5v)D^2x \right. \\ \qquad \left. +(3L-x)x^2\right] \end{cases}, \qquad (20)$$

where E is the elastic modulus, v is the Poisson's ratio, and I is the moment of inertia which is given by $D^3/12$ for a beam with rectangular cross-section and unit thickness. The stresses are

$$\begin{cases} \sigma_{xx} = -\frac{P}{I}(L-x)\left(y-\frac{1}{2}D\right) \\ \sigma_{yy} = 0 \\ \sigma_{xy} = -\frac{P_y}{2I}(y-D) \end{cases}. \qquad (21)$$

This problem is solved with $E=1.0\times 10^3, v=\frac{1}{3}, D=2$ and $L=12$. The displacements given by (20) are applied at all boundary nodes, and 31×11 arrangement of data points is used. Excellent results are obtained by using the globally supported RBFs, as shown in Tables 8 and 9. As mentioned by Liszka [5], very slender domains generally lead to a significant loss of accuracy when collocation

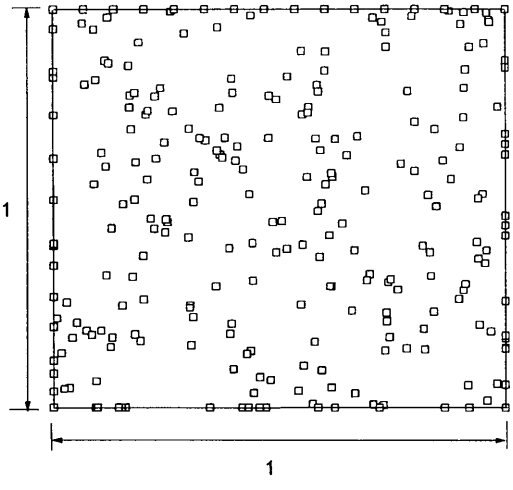

Fig. 8. Randomly distributed 256 nodes discretization

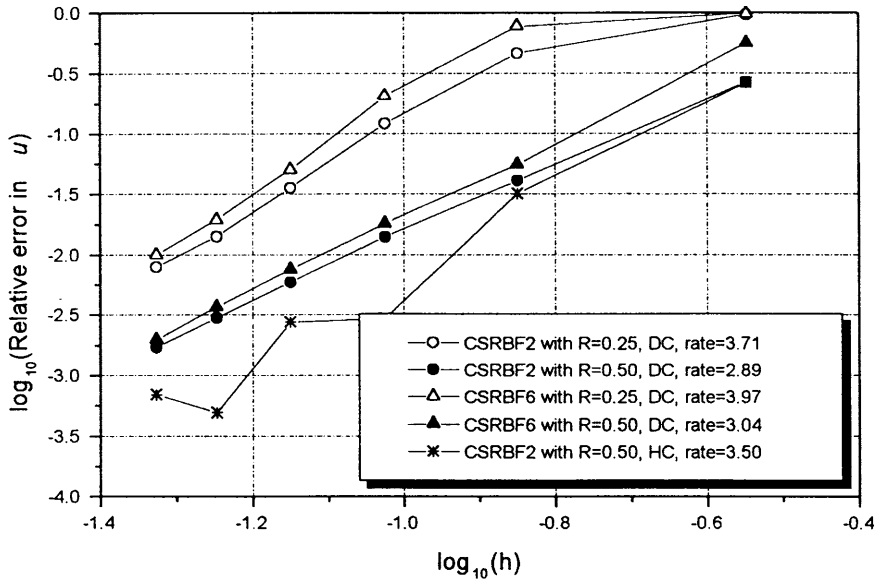

Fig. 9. Convergence rates in u for compactly supported RBFs

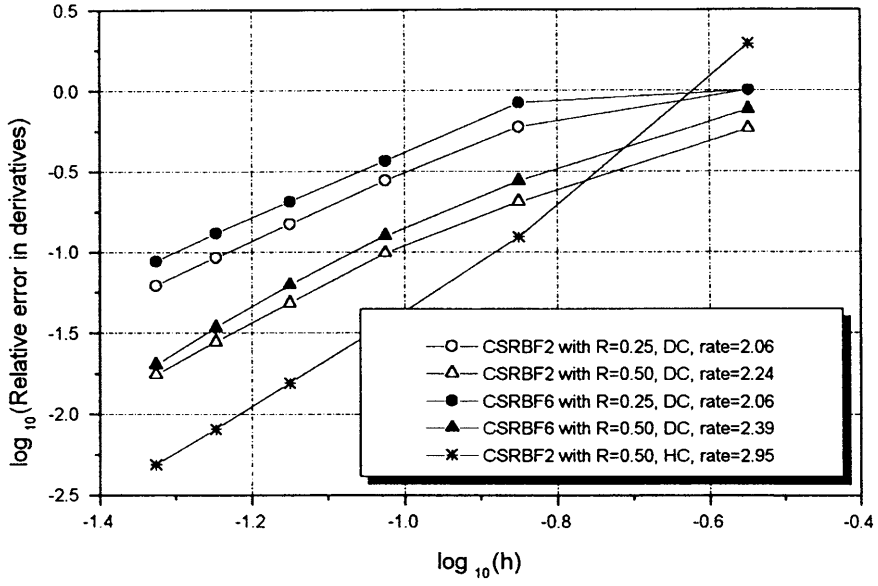

Fig. 10. Convergence rates in derivatives for compactly supported RBFs

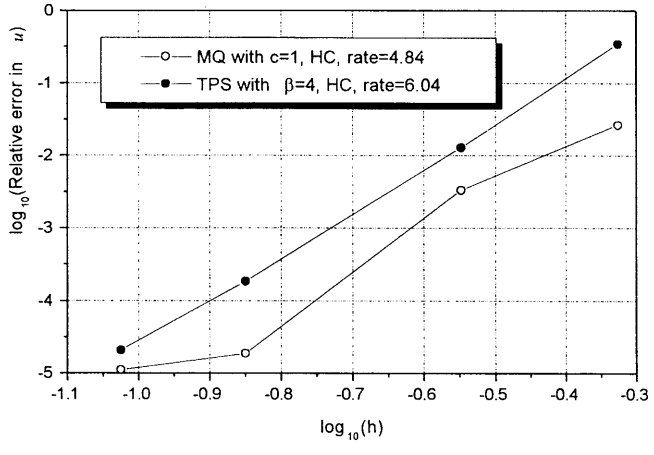

Fig. 11. Convergence rates for globally supported RBFs

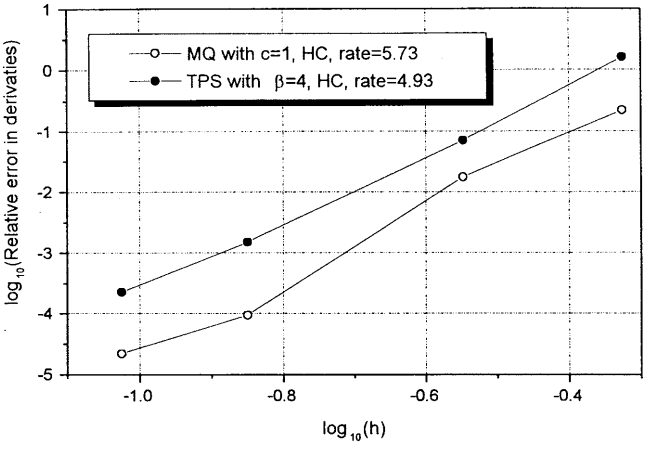

Fig. 12. Convergence rates in derivatives for globally supported RBFs

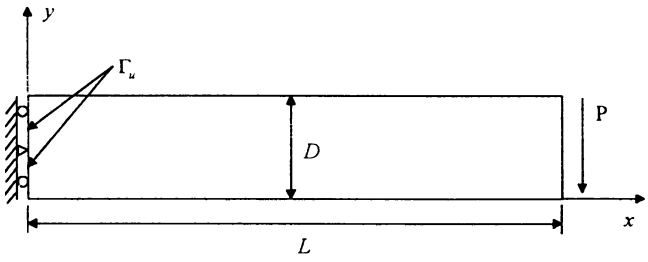

Fig. 13. Cantilever beam

method is used. In this numerical example, the beam is a slender domain, so it results in significant error in stresses when the compactly supported RBFs are used, as shown in Tables 8 and 9. Even so, excellent accuracy is still obtained for displacement. Numerical results show that the Hermite type collocation improve the accuracy significantly.

4.3
Plate with a hole

Consider the problem of an infinite plate with a hole of radius a loaded infinity by a traction σ_0 in the x direction. The analytical solution of this problem is given by

$$\begin{cases} \sigma_x(x,y) = \sigma_0\left\{1 - \frac{a^2}{r^2}\left(\frac{3}{2}\cos 2\theta + \cos 4\theta\right) + \frac{3a^4}{2r^4}\cos 4\theta\right\} \\ \sigma_y(x,y) = -\sigma_0\left\{\frac{a^2}{r^2}\left(\frac{1}{2}\cos 2\theta - \cos 4\theta\right) - \frac{3a^4}{2r^4}\cos 4\theta\right\} \\ \tau_{xy}(x,y) = -\sigma_0\left\{\frac{a^2}{r^2}\left(\frac{1}{2}\sin 2\theta + \sin 4\theta\right) + \frac{3a^4}{2r^4}\sin 4\theta\right\} \end{cases}, \tag{22}$$

$$\begin{cases} u_r = \frac{\sigma_0}{4G}\left\{r\left[\frac{\kappa-1}{2} + \cos 2\theta\right] + \frac{a^2}{r}\left[1 + (1+\kappa)\cos 2\theta\right] - \frac{a^4}{r^3}\cos 2\theta\right\} \\ u_\theta = \frac{\sigma_0}{4G}\left\{(1-\kappa)\frac{a^2}{r} - r - \frac{a^4}{r^3}\right\}\sin 2\theta \end{cases}, \tag{23}$$

Table 8. Relative error by using direction collocation (%)

	R	CSRBF2	CSRBF6	MQ with $c = 6$	TPS with $\beta = 4$
E_2	2.0	0.64	1.05	6.0×10^{-5}	1.0×10^{-4}
	4.0	0.09	0.12		
	6.0	0.02	0.03		
	8.0	0.01	0.01		
D_2	2.0	465	740	0.0036	0.074
	4.0	58.1	80.0		
	6.0	16.4	18.9		
	8.0	6.71	6.52		

Table 9. Relative error by using Hermite type collocation (%)

	R	CSRBF2	CSRBF6	MQ with $c = 6$	TPS with $\beta = 4$
E_2	2.0	0.31	0.41	1.0×10^{-4}	1.1×10^{-5}
	4.0	0.025	0.023		
	6.0	0.006	0.0046		
	8.0	0.0026	0.0015		
D_2	2.0	334	521	0.0045	0.013
	4.0	34.5	32.7		
	6.0	10.3	6.78		
	8.0	4.39	2.25		

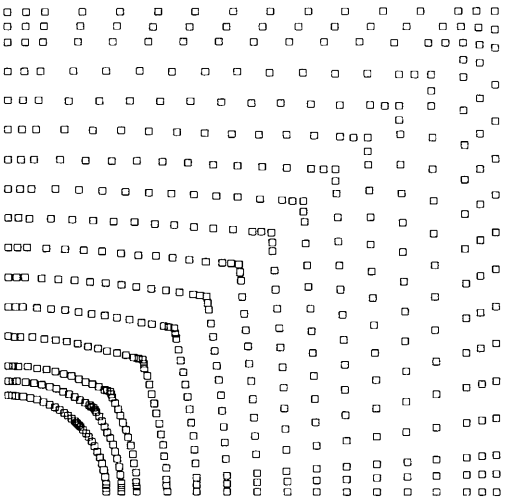

Fig. 14. Nodes discretization

where

$$G = \frac{E}{2(1+\nu)}, \quad \kappa = \begin{cases} 3 - 4\nu & \text{plane strain} \\ \frac{3-\nu}{1+\nu} & \text{plane stress} \end{cases}$$

and (r, θ) is a polar coordinate system with the origin at the center of the hole.

Two cases are analyzed. In the first case, the displacements given by (23) are applied at all boundary nodes of a finite plate with dimensions 5×5 and with a hole of radius $a = 1$, while in the second case, the displacements are only applied at the left and lower edges, and the tractions associated with the stress field given by (22) are applied at the upper and right edges of the same finite plate. In the second case, the inner boundary is traction free boundary. Due to symmetries only the upper right quadrant is modeled. A plane stress state is assumed with material properties $E = 1000$ and $\nu = 1/3$.

Nodes discretization used in this example is shown in Fig. 14, and stresses σ_{xx} at stations along y axis for case 1 obtained by using direct collocation method with RBFs are compared with those obtained by using FEM in Fig. 15. In the FE analysis, quadrilateral finite elements are constructed from the nods shown in Fig. 14. Figure 15 shows that the direct collocation with compactly supported RBFs gives satisfactory results for case 1, and their accuracy is higher than that of FEM. Figures 16 and 17 present stress σ_{xx} at stations along y-axis for case 2 by using direct collocation and Hermite type collocation, respectively, which show that the Hermite type collocation method gives much better results than the direct collocation. Convergence rates are presented in Figs. 18–21, which show that the convergence rates for the Hermite type collocation are much higher than those for the direct collocation.

5
Concluding remarks

Meshless methods based on the direct collocation and the Hermite type collocation are investigated in this paper. This study shows that the direct collocation method leads to significant error in solving PDEs with Neumann

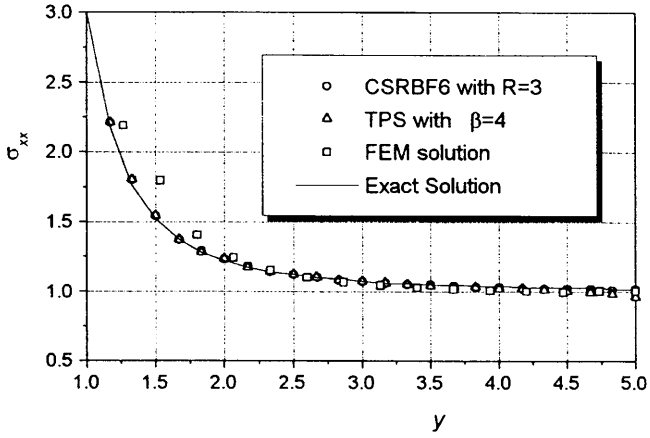

Fig. 15. Stress σ_{xx} at stations along y axis for case 1 by using direct collocation method

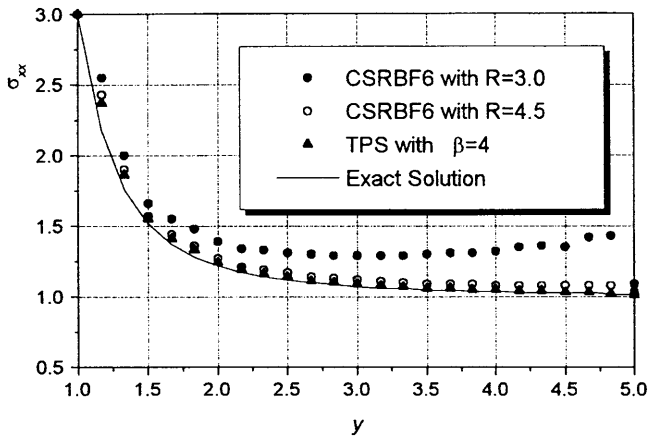

Fig. 16. Stress σ_{xx} at stations along y axis for case 2 by using direct collocation method

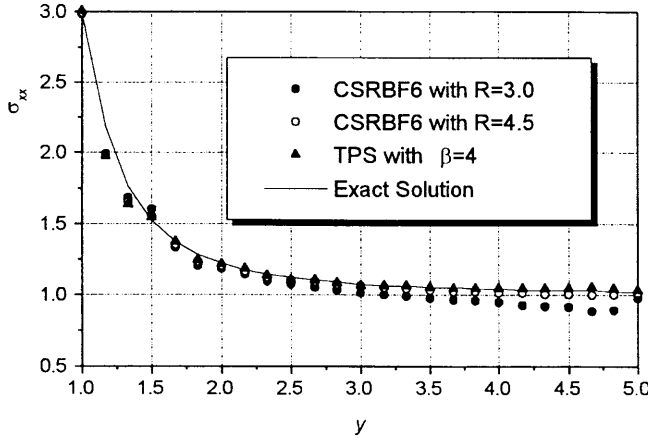

Fig. 17. Stress σ_{xx} at stations along y axis for case 2 by using Hermite based collocation method

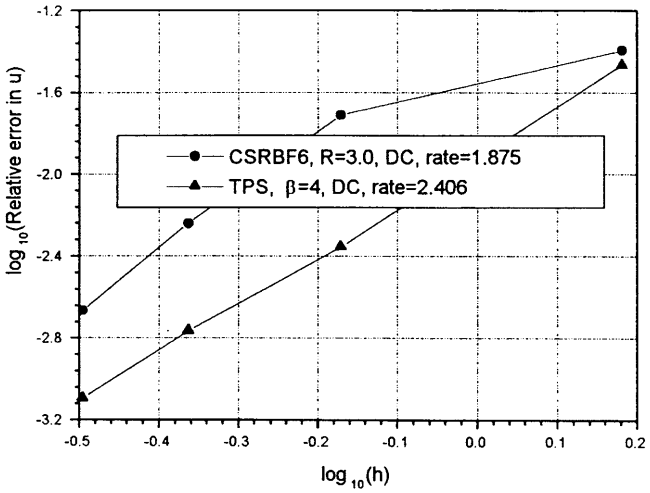

Fig. 18. Convergency rate in displacement for case 1 by using direct collocation method

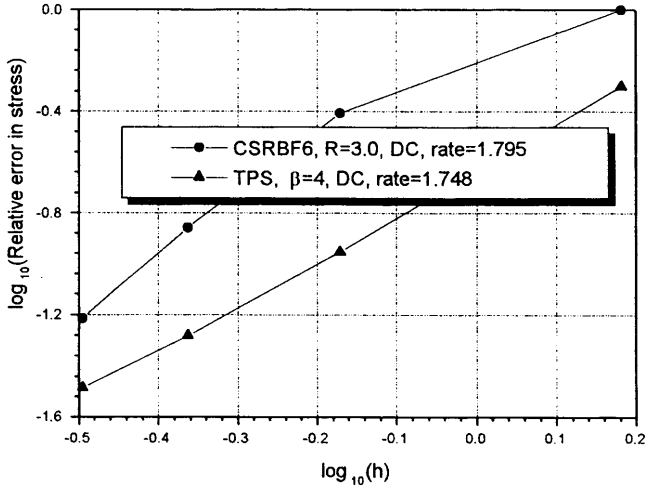

Fig. 19. Convergency rate in stress for case 1 by using direct collocation method

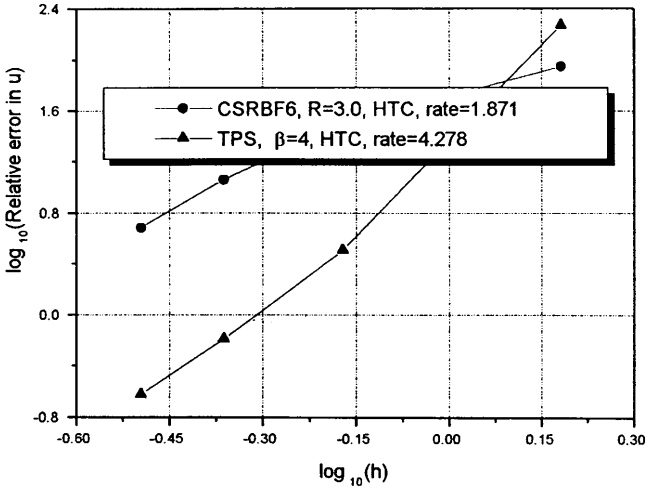

Fig. 20. Convergency rate in displacement for case 2 by using Hermite based collocation method

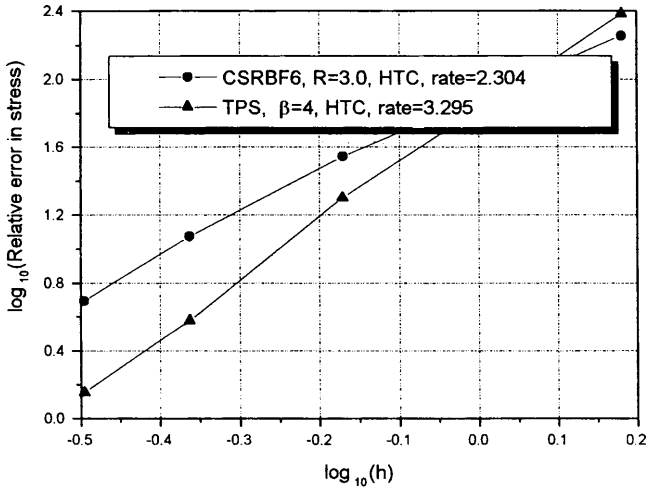

Fig. 21. Convergency rate in stress for case 2 by using Hermite based collocation method

boundary conditions, and the Hermite collocation method proposed in this paper improves the accuracy of solution significantly.

Numerical studies also show that the globally supported RBFs perform excellent in solving PDEs with collocation method, but it leads to a full coefficient matrix. For engineering application, the compactly supported RBFs are recommended, which can obtain reasonable accuracy of results while reduces computational effort required significantly.

Meshless methods based on collocation are truly meshfree methods, and computational effort required is also much less than that required for Galerkin-based meshless methods. However, the accuracy of the collocation method is less than that of the Galerkin method, therefore more nodes are needed for the collocation method than that needed for the Galerkin method to obtain reasonable accuracy of results.

References

1. **Gingold RA, Moraghan JJ** (1977) Smoothed particle hydrodynamics: theory and applications to non-spherical stars. Man. Not. Astrou. Soc. 181: 375–389
2. **Belytschko T, Lu Y, Gu L** (1994) Element free Galerkin methods. Int. J. Numer. Methods Engrg. 37: 229–256
3. **Liu WK, Jun S, Zhang YF** (1995) Reproducing kernel particle methods. Int. J. Numer. Methods Fluids 20: 1081–1106
4. **Oñate E, Idelsohn S, Zienkiewicz OC, Taylor RL** (1996) A finite point method in computational mechanics. Applications to convective transport and fluid flow. Int. J. Numer. Methods Engrg. 39: 3839–3866
5. **Liszka TJ, Duarte CAM, Tworzydlo WW** (1996) hp-meshless cloud method. Comput. Methods Appl. Mech. Engrg. 139: 263–288
6. **Atluri SN, Zhu TL** (2000) The meshless local Petrov-Galerkin (MLPG) approach for solving problems in elasto-statics. Comput. Mech. 25: 169–179
7. **Atluri SN, Zhu TL** (2000) New concepts in meshless methods. Int. J. Numer. Meth. Engrg. 47: 537–556
8. **Atluri SN, Kim HG et al** (1999) A critical assessment of the truly Meshless Local Petrov-Galerkin (MLPG), and Local Boundary Integral Equation (LBIE) methods. Comput. Mech. 24: 348–372
9. **Atluri SN, Zhu T**(1998) A new meshless local Petrov-Galerkin (MLPG) approach in computational mechanics. Comput. Mech. 22: 117–127
10. **Atluri SN, Sladek J et al** (2000) The local boundary integral equation (LBIE) and it's meshless implementation for linear elasticity. Comput. Mech. 25: 180–198
11. **Zhu T, Zhang JD, Atluri SN** (1998) A local boundary integral equation (LBIE) method in computational mechanics, and a meshless discretization approach. Comput. Mech. 21: 223–235
12. **Krongauz Y, Belytschko T** (1996) Enforcement of essential boundary conditions in meshless approximations using finite elements. Comput. Methods Appl. Mech. Engrg. 131: 133–145
13. **Gosz J, Liu WK** (1996) Admissible approximations for essential boundary conditions in the reproducing kernel particle method. Comput. Mech. 19: 120–135
14. **Zhu T, Atluri SN** (1998) Modified collocation method and a penalty formulation for enforcing the essential boundary conditions in the element free Galerkin method. Comput. Mech. 21: 211–222
15. **Mukherjee YX, Mukherjee S** (1997) On boundary conditions in the element free Galerkin method. Comput. Mech. 19: 267–270
16. **Zhang X, Liu X, Lu M-W, Chen Y** Imposition of essential boundary conditions by displacement constraint equations in meshless methods (submitted to Int. J. Numer. Methods Engrg.)
17. **Frank R** (1972) Scattered data interpolation: tests of some methods. Math. Comput. 38: 181–199
18. **Hardy RL** (1971) Multiquadric equations of topography and other irregular surfaces. J. Geophys. Res. 76: 1905–1915
19. **Wu Z** (1992) Hermite-Birkhoff interpolation of scattered data by radial basis functions. Approx. Theory Appl. 8: 1–10
20. **Kansa EJ** (1990) Multiquadrics – a scattered data approximation scheme with applications to computational fluid dynamics – I. Surface approximations and partial derivative estimates. Comput. Math. Appl. 19(8/9): 127–145
21. **Kansa EJ** (1990) Multiquadrics – a scattered data approximation scheme with applications to computational fluid dynamics – II. Solutions to hyperbolic, parabolic, and elliptic partial differential equations. Comput. Math. Appl. 19(8/9): 147–161
22. **Sharan M, Kansa EJ, Gupta S** (1997) Applications of the multiquadric method for the solution of elliptic partial differential equations. Appl. Math. Comput. 84: 275–302
23. **Fasshauer GE** (1996) Solving partial differential equations by collocation with radial basis functions. In: LeMéhauté A, Rabut C, Schumaker LL (eds.) Chamonix proceedings. Vanderbilt University Press, Nashville, TN, pp. 1–8
24. **Wu Z, Schaback R** (1993) Local error estimates for radial basis function interpolation of scattered data. IMA J. Numer. Anal. 13: 13–27
25. **Wu Z** (1998) Solving PDE with radial basis function and the error estimation. In: Chen Z, Li Y, Micchelli CA, Xu Y, Dekker M, GuangZhou (eds.) Advances in Computational Mathematics Lecture Notes on Pure and Applied Mathematics, pp. 202
26. **Franke C, Schaback R** (1998) Solving partial differential equations by collocation using radial basis functions. Appl. Math. Comput. 93: 73–82
27. **Wong SM, Hon YC, Li TS, Chung SL, Kansa EJ** (1999) Multizone decomposition of time-dependent problems using the multiquadric scheme. Comput. Math. Appl. 37(8): 23–43
28. **Wu Z** (1995) Compactly supported positive definite radial functions. Adv. Comput. Math. 4: 283–292
29. **Wendland H** (1995) Piecewise polynomial, positive definite and compactly supported radial basis functions of minimal degree. Adv. Comput. Math. 4: 389–396
30. **Buhmann MD** (1998) Radial functions on compact support. Proc. Edinburgh Math. Soc. 41: 33–46

31. Micchelli CA (1986) Interpolation of scattered data: distance matrices and conditionally positive definite functions. Constr. Approx. 2: 11–22
32. Powell MJD (1987) Radial basis functions for multivariable interpolation, a review. In: Griffiths DF, Watson GA (eds.). Numerical Analysis. Longman Scientific & Technical, Harlow, pp. 223–241
33. Timoshenko SP, Goodier JN (1987) Theory of Elasticity, 3rd edn,. McGraw-Hill, New York